Article

Chinese Science Bulletin

Condensed Matter Physics

January 2011 Vol.56 No.2: 137–141
doi: 10.1007/s11434-010-4217-x

Preparation and luminescence properties of monodisperse silica/aminosilane-coated Y_2O_3:Yb,Ho upconversion nanoparticles

PANG Tao, CAO WangHe*, XING MingMing, LUO XiXian & XU ShuJing

Optoelectronic Technology Institute, Dalian Maritime University, Dalian 116026, China

Received May 6, 2010; accepted July 13, 2010

Monodisperse silica/aminosilane-coated Y_2O_3:Yb,Ho nanoparticles are prepared via homogenous precipitation combined with a polyvinylpyrrolidone-assisted ammoniation method. The factors that contribute to the success of the coating are examined, and the procedure is optimized. Compared with uncoated nanoparticles, coated nanoparticles exhibit an increased ratio of green to red emission intensity, which can mainly be attributed to the decreased number of surface defects induced by the surface coating.

silica coating, yttrium oxides, nanoparticles, upconversion luminescence

Citation: Pang T, Cao W H, Xing M M, et al. Preparation and luminescence properties of monodisperse silica/aminosilane-coated Y_2O_3:Yb,Ho upconversion nanoparticles. Chinese Sci Bull, 2011, 56: 137–141, doi: 10.1007/s11434-010-4217-x

Upconversion luminescence is a physical process where low frequency light is converted to high frequencies via multi-photon absorption [1]. Due to potential applications in solid state lasers, three dimensional displays and anti-forgery, considerable effort has been devoted to the study of upconversion luminescence since the concept was first formulated by Auzel in the mid-1960s [1–5]. Recently, fluorescent bioprobes based on upconversion nanocrystals have attracted much attention because they not only overcome the inherent disadvantages of conventional fluorescence markers such as photobleaching, optical damage and auto- fluorescence, but also allow *in vivo* imaging of deep tissues [6–11].

Yttria-based upconversion nanocrystals (YUNs) are well known as an excellent candidates for upconversion fluorescent bioprobes because of their favorable chemical and thermal stability, nontoxicity and high emissive intensity [12–21]. However, unmodified YUNs tend to agglomerate in water and lack surface groups capable of coupling biomolecules, which limits their application in bioassays. Various methods have been developed to solve these problems [17–21], among which surface coating the YUNs with silica and/or siloxane layers is the simplest and effective method. To date, the silica or silica/siloxane layers coated on the aggregated YUNs are relatively thick (more than 20 nm), and the particles coated are larger than 100 nm. However, it has been reported that ideal fluorescence biolabeling materials should be well-dispersed nanoparticles coated with thin shells [22].

In this paper, silica/aminosilane-coated Y_2O_3:Yb,Ho (Y-Y-H) nanoparticles with cores that are about 40 nm in diameter and shells of about 5 nm in thickness were prepared via a modified homogenous precipitation method combined with a polyvinylpyrrolidone (PVP)-assisted ammoniation process. The factors playing key roles in achieving a thin coating, and the effects of the coating on the upconversion luminescence of the Y-Y-H nanoparticles are investigated.

1 Experimental

1.1 Materials

AR grade urea, absolute ethanol, ammonia (25 wt%–28 wt%), tetraethoxysilane (TEOS), 3-aminopropyltriethoxysi-

*Corresponding author (email: whcao@online.ln.cn)

lane (APES), and PVP (k-30) were used in the experiments. Rare-earth nitrate stock solutions were prepared from the corresponding oxides (purity 99.99%).

1.2 Particle Characterization

Transmission electron microscopy (TEM) was carried out on a Tecnai G2 20 microscope. Fourier transform infrared (FTIR) spectra over the range 400–4000 cm^{-1} were obtained on a Magna-IR 550 spectrometer using KBr pellets (the weight ratio of sample to KBr was 1%). Upconversion spectra were recorded on a Hitachi F-4500 fluorescence spectrometer equipped with a 980 nm continuous wave laser diode (LD).

1.3 Synthesis of Y-Y-H nanoparticles

A procedure from [23] was modified to prepare Y_2O_3 nanoparticles doped with 6% Yb and 1.5% Ho. An aqueous solution containing rare-earth nitrates (0.01 mol/L) was made by mixing stoichiometric amounts of $Y(NO_3)_3$, $Yb(NO_3)_3$ and $Ho(NO_3)_3$ stock solutions, followed by dilution with water. Similarly, an identical volume of an aqueous solution of urea (6 mol/L) was also made. The two solutions were mixed and then aged at 83°C for 9 min. The resulting white precipitate was collected by filtration, washed three times with water and ethanol, and then dried at 40°C for 12 h. Finally, the Y-Y-H nanoparticles were obtained by firing the white precipitate at 800°C for 1 h.

1.4 Synthesis of individually silica/aminosilane-coated Y-Y-H nanoparticles

Silica/aminosilane-coated Y-Y-H nanoparticles were prepared by PVP-assisted ammoniation. In a typical procedure, Y-Y-H nanoparticles (0.06 g) were dispersed in a solution of ethanol (50 mL) containing PVP (0.3 g), water (5 mL) and ammonia (4 mL) using an ultrasonic bath. The suspension was then stirred magnetically at room temperature and a solution of TEOS (0.04 mL) in ethanol (20 mL) was added. After 3 h, a solution of APES (0.04 mL) in ethanol (20 mL) was added and the reaction was stirred for an additional 1 h. The resulting product (Y-Y-H/S-N2) was precipitated using a centrifuge, washed three times with ethanol and then redispersed in ethanol. For comparison, Y-Y-H/S1, Y-Y-H/S2, Y-Y-H/S3 and Y-Y-H/S-N1 samples were also prepared. The details of the conditions used are presented in Table 1.

2 Results and discussion

TEM images of Y-Y-H, Y-Y-H/S1, Y-Y-H/S2, Y-Y-H/S3, Y-Y-H/S-N1 and Y-Y-H/S-N2 are shown in Figure 1. TEM observation showed that the Y-Y-H nanoparticles are well dispersed and have diameters of about 40 nm. In contrast, the Y-Y-H/S1 nanoparticles form a micrometer-sized aggregate of crystallites with diameters of 40 nm. In fact, we concluded that the Y-Y-H/S1 nanoparticles aggregate without the need for TEM observation because they settle out of the reaction solution after only 10 min. According to [24], Y-Y-H nanoparticles are very unstable under the coating conditions, resulting in a tendency to aggregate. Thus the most important requirement for preparing monodisperse silica-coated Y-Y-H nanoparticles is to prevent the aggregation of Y-Y-H during silica coating. Adsorbing PVP onto Y-Y-H prior to silica coating appears to be a good method for preventing aggregation because (1) PVP can adsorb onto a broad range of different materials, (2) PVP has a larger hydrodynamic radius than Y-Y-H, which can offer sufficient steric hindrance to prevent the flocculation of Y-Y-H, and (3) the adsorption of PVP onto Y-Y-H aids the deposition of silica onto Y-Y-H [22,25–29]. As expected, monodisperse Y-Y-H/S2 was obtained by prior addition of PVP. The silica shells are difficult to observe because Y-Y-H/S2 is an unwashed sample that includes large amounts of core-free silica particles. In the studies of other silica-coated materials (e.g. magnetic materials), researchers proved that the secondary nucleation of silica can be avoided by carefully controlling the process parameters (including reaction temperature, reaction time, ratio of TEOS to core particles, and the content of water and/or ammonia). However, the optimum parameters are not universal because the nanoparticles vary in size and morphology as well as in their physical and chemical properties. In other words, it is necessary to optimize the procedure for each new material, which inevitably increases the testing cost and prolongs the experimental period. There exists a need to develop a simple but effective method that will allow the secondary nucleation of silica particles to be avoided when applying silica coatings

Table 1 Samples coated under different conditions

Sample	Water (mL)	Ammonia (mL)	TEOS (mL)	APES (mL)	PVP (g)	Y-Y-H (g)	Product collection
Y-Y-H/S1	5	4	0.16			0.06	settled for 10 min
Y-Y-H/S2	5	4	0.16		0.3	0.06	reaction solution
Y-Y-H/S3	5	4	0.16		0.3	0.06	centrifugation
Y-Y-H/S-N1	5	4	0.16	0.16	0.3	0.06	centrifugation
Y-Y-H/S-N2	5	4	0.04	0.04	0.3	0.06	centrifugation

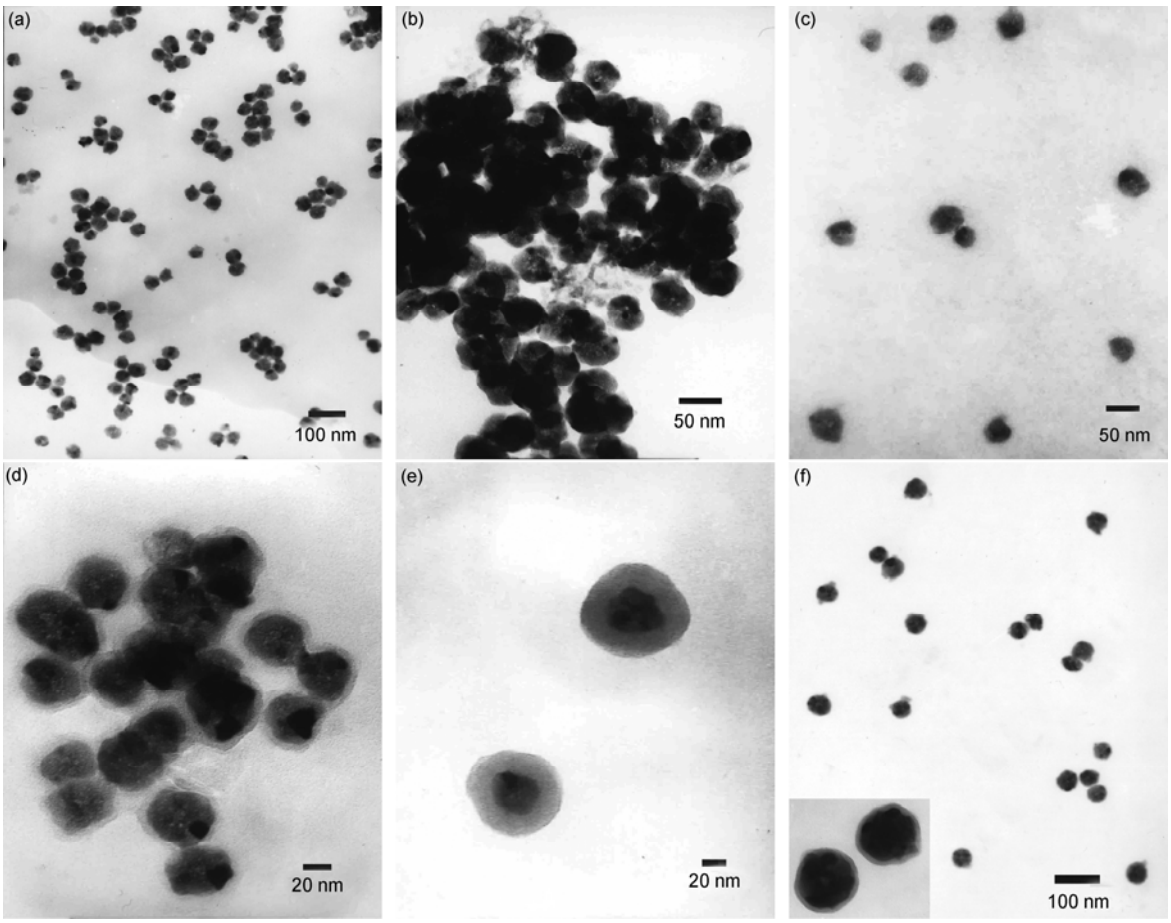

Figure 1 TEM images of Y-Y-H (a), Y-Y-H/S1 (b), Y-Y-H/S2 (c), Y-Y-H/S3 (d), Y-Y-H/S-N1 (e) and Y-Y-H/S-N2 (f). Inset: magnified image of Y-Y-H/S-N2 particles.

to nanoparticles. Considering the large difference in size between the Y-Y-H/S2 and silica particles, centrifugation was used to remove the silica particles. However, centrifugation results in the aggregation of Y-Y-H/S2 (Figure 1(d)) and redispersion did not occur even after a long period in an ultrasonic bath. This indicates that the silica-coated particles have been linked by the condensation of hydroxyl groups. Addition of ammonia is a feasible solution to shield the hydroxyl groups from condensation because it bypasses the need for removing silica-coated particles and grafts $-NH_2$ groups onto the silica-coated particles. Figure 1(e) and (f) show the TEM images of Y-Y-H/S-N1 and Y-Y-H/S-N2, respectively, that were prepared using the PVP-assisted ammoniation method. Clearly, monodisperse silica/aminosilane-coated Y-Y-H nanoparticles have been obtained; in addition, no core-free silica particles are found. The different coating thickness between Y-Y-H/S-N1 and Y-Y-H/S-N2 is attributed to the different amounts of TEOS and APES added, which indicates that the coating thickness can be controlled easily in this manner. The thickness of the coating decreases from ~20 to ~5 nm when the amounts of both TEOS and APES are decreased from 0.16 to 0.04 mL.

To further confirm that the silica/aminosilane layers have been coated on the surface of the Y-Y-H nanoparticles, FTIR spectra of the Y-Y-H and Y-Y-H/S-N2 nanoparticles were measured (Figure 2). In the FTIR spectrum of Y-Y-H, the wide bands at 3400 and 1513 cm^{-1} correspond to OH^- and CO_3^{2-}, respectively, while the peaks at 564 and 462 cm^{-1} result from the vibration of Y-O. In the case of Y-Y-H/S-N2, some extra bands are observed in addition to the above peaks. These correspond to N-H (3251 cm^{-1}), C-H (2955 cm^{-1}), C-N (1662 cm^{-1}) and Si-O-Si (1082 cm^{-1}) modes. This indicates that silica/aminosilane layers have been coated on the Y-Y-H nanoparticles.

Because thick shells will prevent upconversion nanocrystals from behaving as bioprobes [22], only the effect of thin shells on the luminescence properties of Y-Y-H has been investigated. As shown in Figure 3, Y-Y-H and Y-Y-H/S-N2 exhibit two bands when excited at 980 nm with a LD. The green emission at 548 nm corresponds to the $^5F_4/^5S_2 \rightarrow {}^5I_8$ transition, while the red emission at 666 nm results from the $^5F_5 \rightarrow {}^5I_8$ transition. It is interesting that the ratio of the intensity of the green to red emission (I_g/I_r) increases from ~0.78 (Y-Y-H) to ~1.15 (Y-Y-H/S-N2) after addition of the silica/aminosilane coating. The green and red emission intensities are proportional to the population of

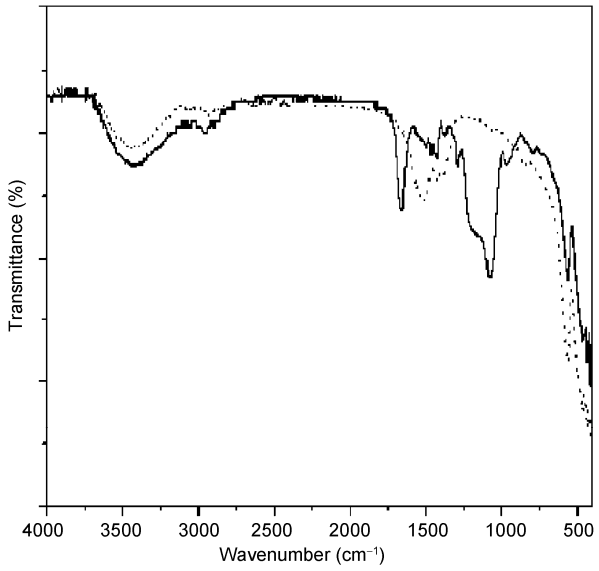

Figure 2 FTIR spectra of Y-Y-H (dotted line) and Y-Y-H/S-N2 nanoparticles (solid line).

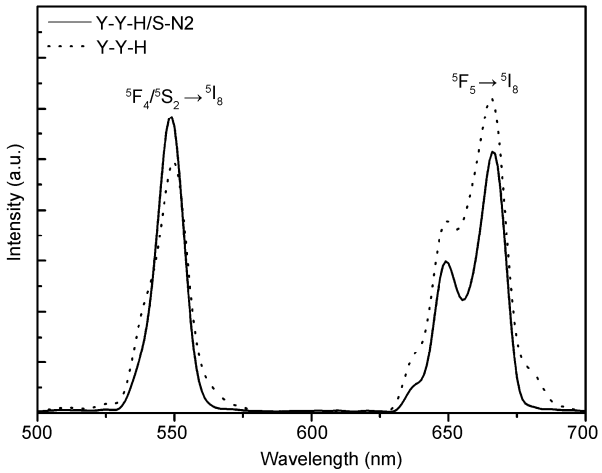

Figure 3 Upconversion spectra of Y-Y-H and Y-Y-H/S-N2 upon excitation at 980 nm with a LD.

the $^5F_4/^5S_2$ and $^5F_5$ states, respectively, and thus the change of I_g/I_r suggests that the coating affects the population of the $^5F_4/^5S_2$ and $^5F_5$ levels. It is well known that at low concentrations of Ho^{3+} ions, a two-step energy transfer process from Yb^{3+} to Ho^{3+} ions is dominant for the Yb^{3+}/Ho^{3+} codoped systems [17]. From the energy level diagram shown in Figure 4, the population of the $^5F_5$ level is mainly dependent on the nonradiative relaxation processes of $^5I_6 \rightarrow {}^5I_7$ and $^5F_4/^5S_2 \rightarrow {}^5F_5$. The smaller the nonradiative relaxation rate, the smaller the population of $^5F_5$ and the larger I_g/I_r will be. Therefore, the increasing I_g/I_r indicates that the silica/aminosilane coating decreases the nonradiative relaxation rates of $^5I_6 \rightarrow {}^5I_7$ and $^5F_4/^5S_2 \rightarrow {}^5F_5$. This can be explained by a decrease in the number of surface defects (i.e. nonradiative relaxation centers) after coating [30,31].

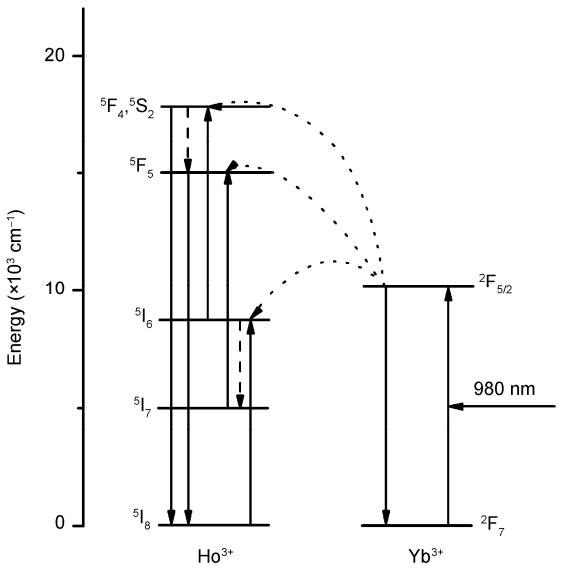

Figure 4 Energy level diagrams for Yb^{3+} and Ho^{3+} ions and possible upconversion mechanisms.

Recently, Lü et al. [20,21] reported that in addition to the decrease of surface defects, a coating could also change the crystal field around the dopant ions at the surface of the nanoparticles. However, it is thought that the silica/aminosilane coating used herein has little influence on the crystal field around the dopant ions at the surface because the position and shape of the emission bands do not change upon addition of the coating (see Figure 3) [32,33]. The reason for this may be that the introduction of PVP weakens the effect of the silica/aminosilane coating on the crystal field around the surface dopant ions.

3 Conclusion

A simple method to prepare monodisperse silica/aminosilane-coated Y-Y-H nanoparticles was reported, and the factors playing key roles in the success of the coating were discussed. The coated Y-Y-H nanoparticles show enhanced I_g/I_r compared with the uncoated counterpart, which was attributed to a decrease in the number of surface defects upon coating.

This work was supported by the National Natural Science Foundation of China (60979003), the Program for New Century Excellent Talents Plan of the Ministry of Education of China (NCET-10-0171) and the Scientific Research Fund of Liaoning Province Education Department (2009A095).

1 Pang T, Cao W H. Upconversion luminescence of Er^{3+} doped and Er^{3+}/Yb^{3+} codoped $YTaO_4$. Chinese Sci Bull, 2008, 53: 178–182
2 Yang Z M, Jiang Z H. Effect of alkali metal oxides on upconversion fluorescence properties of germanate-tellurite glasses. Chinese Sci Bull, 2004, 49: 2572–2574
3 Chen X B, Song Z F. The study of two-color excitation upconversion

of Pr(0.5)Yb(3):ZBLAN. Sci China Ser G-Phys Mech Astron, 2006, 49: 169–177
4 Chen X B, Song Z F, Wu J G, et al. Ultraviolet and visible upconversion luminescence of Tm(0.1)Yb(5):FOV oxyfluoride nanophase vitroceramics. Sci China Ser G-Phys Mech Astron, 2008, 51: 1868–1876
5 Zhao S L, Xu Z, Wang L H, et al. Influence of Yb^{3+} concentration on the upconversion luminescence of oxyfluoride material doped with Er^{3+}. Sci China-Phys Mech Astron, 2010, 53: 310–314
6 Chatterjee D K, Rufaihah A J, Zhang Y. Upconversion fluorescence imaging of cells and small animals using lanthanide doped nanocrystals. Biomaterials, 2008, 29: 937–943
7 Kumar M, Guo Y Y, Zhang P. Highly sensitive and selective oligonucleotide sensor for sickle cell disease gene using photon upconverting nanoparticles. Biosens Bioelectron, 2009, 24: 1522–1526
8 Ehlert O, Thomann R, Darbandi M, et al. A four-color colloidal multiplexing nanoparticle system. ACS Nano, 2008, 2: 120–124
9 Cui L L, Fan H L, Xiao J P, et al. Surface modification of upconversion luminescence material $Na[Y_{0.57}Yb_{0.39}Er_{0.04}]F_4$ with hydrosulfide group. J Univ Sci Tech Beijing, 2008, 15: 605–610
10 Wei Y, Lu F Q, Zhang X R, et al. Synthesis and characterization of efficient near-infrared upconversion Yb and Tm codoped $NaYF_4$ nanocrystal reporter. J Alloy Compd, 2007, 427: 333–340
11 Zeng J H, Su J, Li Z H, et al. Synthesis and upconversion luminescence of hexagonal-phase $NaYF_4$:Yb,Er^{3+} phosphors of controlled size and morphology. Adv Mater, 2005, 17: 2119–2123
12 Lim S F, Riehn R, Ryu W S, et al. *In vivo* and scanning electron microscopy imaging of upconverting nanophosphors in caenorhabditis elegans. Nano Lett, 2006, 6: 169–174
13 Qin X, Yokomori T, Ju Y G. Flame synthesis and characterization of rare-earth (Er^{3+}, Ho^{3+}, and Tm^{3+}) doped upconversion nanophosphors. Appl Phys Lett, 2007, 90: 073104
14 Schubert D, Dargusch R, Raitano J, et al. Cerium and yttriuim oxide nanoparticles are neuroprotective. Bionchem Bioph Res Co, 2006, 342: 86–91
15 Chen G Y, Liu Y, Zhang Y G, et al. Bright white upconvesion luminescence in rare-earth-ion-doped Y_2O_3 nanocrystals. Appl Phys Lett, 2007, 91: 133103
16 Matsuura D, Ikeuchi T, Soga K. Upconversion luminescence of colloidal solution of Y_2O_3 nano-particles doped with trivalent rare-earth ions. J Lumin, 2008, 128: 1267–1270
17 Zhang J, An L Q, Wang S W. Preparation and upconversion luminescence of Y_2O_3:Yb^{3+},Ho^{3+} nanocrystalline powders coated with SiO_2. J Alloys Compd, 2009, 471: 201–203
18 Traina C A, Schwartz J. Surface modification of Y_2O_3 nanoparticles. Langmuir, 2007, 23: 9158–9161
19 Kamimura M, Miyamoto D, Saito Y, et al. Design of poly(ethylene glycol)/streptavidin coimmobilized upconversion nanophosphors and their application to fluorescence biolabeling. Langmuir, 2008, 24: 8864–8870
20 Lü Q, Guo F Y, Sun L, et al. Silica-/titania/coated Y_2O_3:Tm^{3+}/Yb^{3+} nanoparticles with improvent in upconversion luminescence induced by different thickness shells. J Appl Phys, 2008, 103: 123533
21 Lü Q, Li A H, Guo F Y, et al. Experimental study on the surface modification of Y_2O_3:Tm^{3+}/Yb^{3+} nanoparticles to enhance upconversion fluorescence and weaken aggregation. Nanotechnology, 2008, 19: 145701
22 Wang Y, Qin W P, Zhang J S, et al. Synthesis and green upconversion fluorescence of colloidal $La_{0.78}Yb_{0.20}Er_{0.02}F_3/SiO_2$ core/shell nanocrystals. J Solid State Chem, 2007, 180: 2268–2272
23 Matijević E, Hsu W P. Preparation and properties of monodispersed colloidal particles of lanthanide compouds. J Colloid Interface Sci, 1987, 118: 506–523
24 Parks G A. The isoelectric points of solid oxides, solid hydroxides, and aqueous hydroxo complex systems. Chem Rev, 1965, 65: 177–198
25 Smith J N, Meadows J, Williams P A. Adsorption of polyvinylpyrrolidone onto polystyrene lattices and the effect on colloid stability. Langmuir, 1996, 12: 3773–3778
26 Yang Y, Li J R, Mu J, et al. A gold nanocomposite made soluble in both water and oil by the addition of a second adsorption layer of poly-N-vinyl-2-pyrrolidone on gold nanoparticles that have been made hydrophobic. Nanotechnology, 2006, 17: 461–465
27 Esumi K, Matsui H. Adsorption of non-ionic and cationic polymers on silica from their mixed aqueous solutions. Colloid Surface A, 1993, 80: 273–278
28 El-Toni A M, Yin S, Sato T. Control of silica shell thickness and microporosity of titania-silica core-shell type nanoparticles to depress the photocatalytic activity of titania. J Colloid Interface Sci, 2006, 300: 123–130
29 Wang C, Ma Z F, Wang T T, et al. Synthesis, assembly, and biofunctionalization of silica-coated gold nanorods for colorimetric biosensing. Adv Funct Mater, 2006, 16: 1673–1678
30 Li Q, Gao L, Yan D S. Effects of the coating process on nanoscale Y_2O_3:Eu^{3+} powders. Chem Mater, 1999, 11: 533–535
31 Li D, Lv S Z, Zhang J S, et al. Size confinement and surface state effect of Eu^{3+}:Y_2O_3 nanocrystals. Chinese J Lumin, 2000, 21: 134–138
32 Luo X X, Cao W H. Upconversion luminescence of holmium and ytterbium co-doped yttrium oxysulfide phosphor. Mater Lett, 2007, 61: 3696–3700
33 De G, Qin W P, Zhang J S, et al. Upconversion luminescence properties of Y_2O_3:Yb^{3+},Er^{3+} nanostructures. J Lumin, 2006, 119-120: 258–263